



HAL
open science

NMR-based metabolic profiling and discrimination of wild tropical tunas by species, size category, geographic origin, and on-board storage condition

Nathalie Bodin, Aurélien Amiel, Edwin Fouché, Fany Sardenne, Emmanuel Chassot, Laurent Debrauwer, Hervé Guillou, Marie Tremblay-Franco, Cécile Canlet

► To cite this version:

Nathalie Bodin, Aurélien Amiel, Edwin Fouché, Fany Sardenne, Emmanuel Chassot, et al.. NMR-based metabolic profiling and discrimination of wild tropical tunas by species, size category, geographic origin, and on-board storage condition. *Food Chemistry*, 2022, 371, 10.1016/j.foodchem.2021.131094 . hal-03376705

HAL Id: hal-03376705

<https://hal.inrae.fr/hal-03376705v1>

Submitted on 16 Oct 2023

HAL is a multi-disciplinary open access archive for the deposit and dissemination of scientific research documents, whether they are published or not. The documents may come from teaching and research institutions in France or abroad, or from public or private research centers.

L'archive ouverte pluridisciplinaire **HAL**, est destinée au dépôt et à la diffusion de documents scientifiques de niveau recherche, publiés ou non, émanant des établissements d'enseignement et de recherche français ou étrangers, des laboratoires publics ou privés.



Distributed under a Creative Commons Attribution - NonCommercial 4.0 International License

35 **Keywords:** *Metabolomics, High-Resolution ^1H NMR; Highly migratory large pelagic fish; Purse*
36 *seine tuna fisheries; western Indian Ocean; Raw white and red muscles.*

37 1 Introduction

38 Sustainable fisheries management relies on the availability of accurate species-specific catch data
39 and may suffer when reported data of species or fishing area are erroneous or inaccurate (Watson
40 & Pauly, 2001). Moreover, ensuring traceability of fishery products “from ocean to plate” is a
41 major concern for instances and food markets worldwide. For example, with the objectives to
42 achieve a high level of consumers’ health protection and to guarantee their right to information,
43 the European Regulation (No 1169/2011) imposes labelling of fishery products with the
44 commercial and scientific name of the species, the area where the organism was caught, the
45 production methods, and the product’s nutritional characteristics. Nevertheless, differences in
46 quality and price according to species, geographical origin, production/fishing modes, or the life
47 history of the live species and product may lead to mislabelling. Efficient methods to assess
48 fishery products authenticity and origin are thus required to help improving fisheries traceability
49 and sustainability, guaranteeing market transparency, and protecting consumers’ safety and rights
50 (Nielsen et al., 2012).

51 The quality and/or origin of fishery product is mostly determined by its biochemical composition,
52 i.e., metabolite profile. Over the past twenty years, Nuclear Magnetic Resonance (NMR)
53 spectroscopy coupled with multivariate analysis has been applied for determining the metabolite
54 profiles of various kinds of food including fish (Martinez et al., 2005; Picone et al., 2011; Wei et
55 al., 2020). The metabolite content of a given sample constitutes a unique profile for the product
56 of all low molecular weight molecules present in, or excreted by, cells or bacteria. Low molecular
57 weight metabolites in fish tissues include free amino acids, nucleotides and related compounds,
58 peptides, organic bases, sugars and inorganic constituents (Piñeiro et al., 2003). In general, the
59 levels of these metabolites vary according to species, environmental conditions, diet, fish tissue,
60 freshness, stress, and post-mortem storage, handling and processing (Piñeiro et al., 2003;
61 Samuelsson & Larsson, 2008). Moreover, compared to other techniques widely used for
62 metabolic profiling such as mass spectrometry, the use of NMR allows a simpler sample
63 preparation and a higher analysis throughput (Jung et al., 2010). Because NMR analyses produce
64 highly complex datasets, multivariate analyses such as Principal Component Analysis (PCA) and
65 Partial Least Squares-Discriminant Analysis (PLS-DA) have been designed specifically to
66 analyse NMR derived data (Hatzakis, 2019). ¹H NMR spectroscopy is therefore a powerful non-
67 specific high-throughput analytical technique to produce a metabolic profile and identify potential
68 compounds useful in characterizing, discriminating and authenticating the metabolic
69 specifications of a particular fishery product and its quality (Hatzakis, 2019).

70 Tunas are among the most traded and valued fish species, with annual global catch of around 6
71 million tonnes, i.e. 10% of the world's international seafood trade (FAO, 2020). While bluefin
72 tunas are the most highly valued species although representing about 1.2% of total tuna catch, the
73 global tuna fisheries are dominated by three tropical tuna species, i.e. skipjack tuna (*Katsuwonus*
74 *pelamis* -SKJ), yellowfin tuna (*Thunnus albacares* -YFT), and bigeye tuna (*T. obesus* -BET) with
75 51%, 26%, and 8% of the total tuna catch, respectively (FAO, 2020). From the different fishing
76 gears targeting tropical tunas, industrial purse-seine contributes most to global catch, i.e. 69%
77 compared to 12% for pole-and-line, 10% for longline, and 9% for other gears during the period
78 2014 to 2018 (FAO, 2020). Purse seine is the less selective gear both in terms of size and species
79 composition. Indeed, purse-seiners catch a mix of free-swimming schools and schools associated
80 with drifting floating objects leading to the simultaneous catch of the three co-occurring tropical
81 tunas, from early juveniles (<30 cm) to the largest and oldest individuals (>150 cm for YFT and
82 BET) (Fonteneau et al., 2013). While tunas are mixed in the wells in the case of brine-freezing
83 (i.e., salted water refrigerated at around -18°C), they are sorted according to species, size
84 category and quality appearance in the case of deep-freezing (i.e., -40°C dry well) storage. The
85 duration of fish storage follows the length of the purse seiner's trips, which is 6 to 9 weeks in the
86 Indian Ocean. Purse seine tropical tunas are supplied to the factories (i) in deep-frozen form for
87 large YFT and BET (i.e., > 10 kg) classified on board with "high quality grade" and sold mainly
88 in pre-cooked loins, or (ii) in brined form for SKJ, small tunas (i.e., < 10 kg), and the remaining
89 large YFT and BET that are being processed and sold as cans (Table S1). Misidentification of
90 tuna can occur when fish are sorted onboard purse-seine vessels, at unloading and/or at the
91 factories, especially in the case of small YFT and BET with similar morphological features
92 (Pecoraro et al., 2016). This raises the possibility of accidental mislabelling, intentional species
93 substitution, or mixing of valuable fish by less valuable ones in the commercial tuna market,
94 motivated by the difference of market prices between species and/or when catch restrictions on
95 overfished specific tuna species exist such as YFT in the Indian Ocean (IOTC Secretariat, 2019).
96 Moreover, the purse-seine fishery catching tropical tunas throughout the year, the meat quality is
97 likely to be subject to changes depending on the geographical area where the tuna was caught, the
98 related diet available and consumed by the tuna in the area, as well as its age (i.e., size) and
99 reproductive status, all these factors known to influence tuna's muscle biochemical composition
100 (Chassot et al., 2019; Pecoraro et al., 2016; Sardenne et al., 2016a; Sardenne et al., 2017). The
101 changes in tuna meat quality may thus affect the efficiency of processing and/or the nutritional
102 benefits for consumers.

103 Although NMR spectrometry was applied on tuna as early as the 90's, only few studies remain
104 available in the literature, especially dealing with tuna muscles (Jääskeläinen et al., 2019;
105 Medina et al., 2000; Sacchi et al., 1993). In this context, the present study aimed at characterizing
106 and discriminating the ¹H NMR low molecular weight metabolic profiles of the muscles of three
107 co-occurring tropical tuna species, namely skipjack, yellowfin and bigeye tunas, targeted by the
108 purse-seine fishery in the western Indian Ocean. The ¹H NMR spectra of tuna muscles' aqueous
109 extracts were then further analysed using PCA and PLS-DA to test for metabolic differences
110 according to tuna size, on-board freezing storage conditions (brine- vs deep-freezing) and
111 geographical origin. Tuna muscle consists of white (or light) and red (or dark) muscles, the latter
112 representing higher proportions in tuna species compared to other fish (e.g., 6-8% of total body
113 mass) (Dickson, 1995); this is because of the high migratory abilities of tunas and their related
114 high needs for fat, glycogen and myoglobin. Both tuna muscles were thus taken into account in
115 the present study: their ¹H NMR metabolic profiles were characterised and compared, and the
116 influence of each of the factors listed above was tested.

117

118 **2 Material and methods**

119 2.1 Chemicals

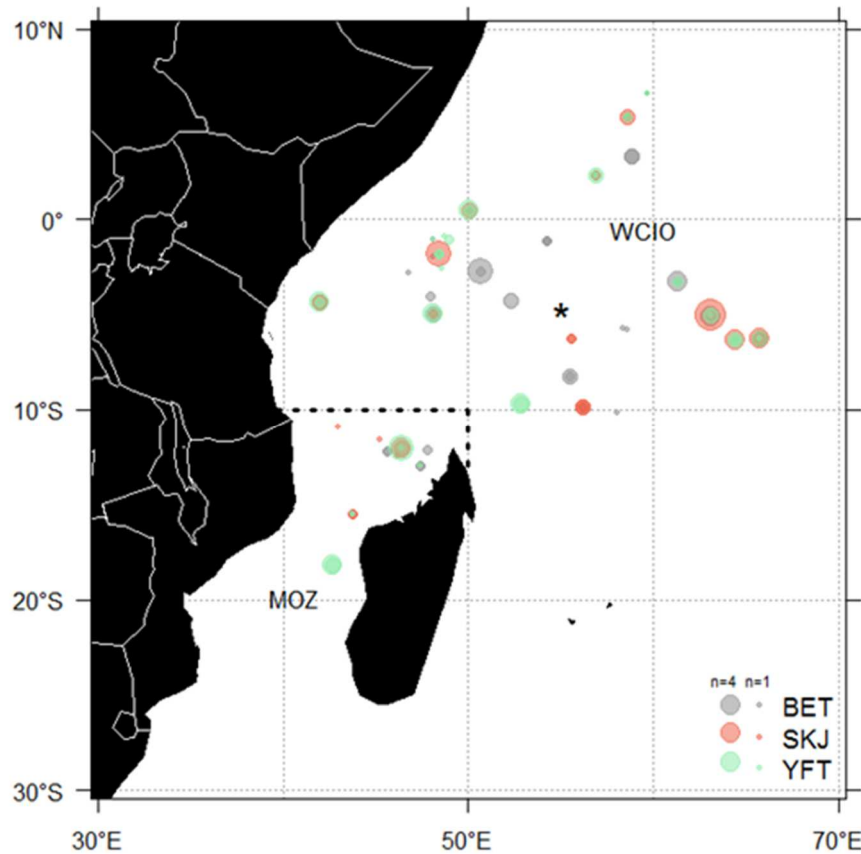
120 Methanol, dichloromethane, ethylene glycol tetra-acetic acid (EgTA) and potassium chloride
121 (KCl) were purchased from Sigma-Aldrich (St Quentin Fallavier, France). Deuterium oxide
122 (D₂O) and sodium 3-trimethylsilyl-2,2,3,3-tetradeuteriopropionate (TMSP) were obtained from
123 Eurisotop (Saint-Aubin, France).

124

125 2.2 Tuna sampling

126 A one-year multi-species sampling was carried out throughout 2013 in the western Indian Ocean.
127 A total of 194 tropical tunas including 60 YFT, 62 BET and 72 SKJ were collected during the
128 unloading of purse seiners at Victoria, Seychelles (Table S1). Fishing date and accurate GPS
129 fishing position from purse seiners' logbooks allowed for the distinction of two main
130 geographical origin areas that differ according to their oceanographic specificities (Chassot et al.,
131 2019): Mozambique Channel (MOZ, n=52) and western-central Indian Ocean (WCIO, n=142)
132 (Fig.1). The onboard storage condition was also recorded during sampling, allowing for the
133 separation between fish stored in brine freezing wells (-18°C) versus those stored in dry deep-
134 freezing wells (-40°C) (Table S1). All sampled fish were weighed (kg to the nearest 0.1 kg), and
135 measured in fork length, which refers to the length from the tip of the snout to the fork of the tail

136 (FL, cm to the nearest 0.5 cm). Then, one sample of around 2 g on a wet weight (ww) basis was
137 taken from the dorsal white muscle (under the dorsal spine on the left side) and a second one
138 from the red muscle (under the pectoral fin on the left side) of each tuna. All samples were stored
139 at $-80\text{ }^{\circ}\text{C}$ until further analyses.



140 **Fig. 1.** Location of yellowfin (YFT, n=60), bigeye (BET, n=62) and skipjack (SKJ, n=72) tuna caught by
 141 purse seine vessels in the western Indian Ocean throughout 2013. The limit of the two geographical origin
 142 areas, Mozambique Channel (MOZ) and western-central Indian Ocean (WCIO) is indicated with dashed
 143 line. Star indicates Port Victoria, Seychelles.
 144
 145

146 **2.3 Sample preparation**

147 A total of 388 samples of tunas' white and red muscles (from 194 tunas) were processed for the
 148 analysis of ^1H NMR Spectroscopy. Approximately 100 ± 0.1 mg ww of each tissue was weighed,
 149 crushed with 1 mL of methanol:ethylene glycol tetraacetic acid (EgTA) (5 mM in water) (2/1,
 150 v/v) using a FastPrep System[®] (MP Biomedicals, Illkirch, France), and extracted with 2 mL of
 151 dichloromethane:methanol (2:1, v/v). After addition of 0.2 volume of aqueous potassium chloride
 152 (KCl) (0.9% w/v), the extracts were further vortexed and centrifuged at 5000g for 10 min, then
 153 the lipid supernatants were removed, while the aqueous extracts were freeze-dried. The resulting
 154 powders were reconstituted in 700 μL of deuteriumoxide (D_2O) in which sodium 3-trimethylsilyl-
 155 2,2,3,3-tetradeuteriopropionate (TMSP; as a chemical shift reference at 0 ppm; 1 mM) was
 156 added. Each sample was vortexed and centrifuged for 10 min, 4°C at 5000g to remove any
 157 precipitate. Then, 600 μL aliquots were transferred to standard 5 mm - NMR tubes (Norell ST
 158 500, Landisville, NJ) for analysis.

159

160 2.4 ¹H NMR Analysis

161 The ¹H-NMR spectra were obtained on a Bruker DRX-600-Avance NMR spectrometer (Bruker,
162 Wissembourg, France) operating at 600.13 MHz for ¹H resonance frequency using an inverse
163 detection 5mm ¹H-¹³C-¹⁵N cryoprobe attached to a CryoPlatform (the preamplifier cooling unit).
164 The ¹H-NMR spectra were acquired at 300K using the Carr-Purcell-Meiboom-Gill (CPMG) spin-
165 echo pulse sequence with pre-saturation, with a total spin echo delay ($2\pi\tau$) of 240ms to attenuate
166 broad signals from proteins and lipoproteins. A total of 128 transients were collected in 32,000
167 data points using a spectral width of 20 ppm, a relaxation delay of 2 sec, and an acquisition time
168 of 1.36 sec. The spectra were Fourier transformed by multiplication of the FIDs by an
169 exponential weighting function corresponding to a line-broadening of 0.3Hz. All spectra were
170 manually phased and baseline corrected and referenced to TMS using Bruker TopSpin 2.1
171 software (Bruker, GMBH, Karlsruhe, Germany). To confirm the chemical structure of
172 metabolites of interest, 2D ¹H-¹H COSY (Correlation Spectroscopy) and 2D ¹H-¹³C-HSQC
173 (Heteronuclear Single Quantum Coherence Spectroscopy) NMR experiments were performed on
174 selected samples. Spectral assignment was based on matching 1D and 2D data to reference
175 spectra in a home-made reference database, as well as with other databases
176 (<http://www.brmb.wisc.edu> and <http://www.hmdb.ca>), and reports in the literature. Absolute
177 concentrations of the metabolites were calculated from the integrals of the TMS signal (known
178 concentration standard) and, the metabolite signal (unknown concentration) as described in
179 (Amiel et al., 2020).

180

181 2.5 Data reduction and multivariate statistical analyses

182 Data were reduced using the AMIX software (version 3.9, Bruker, Rheinstetten, Germany) to
183 integrate variable wide regions corresponding to the δ 9.0-0.90 ppm region for aqueous white and
184 red muscle extracts. A total of 64 and 78 NMR buckets were selected for white muscle and red
185 muscle respectively, according to resonance signals and multiplicity between 9.0 and 0.9 ppm.
186 Regions corresponding to noise or residual water, methanol and dichloromethane were not
187 selected. To account for differences in sample amount, each integrated region was normalized to
188 the total spectral area.

189 Multivariate analyses were used to study the effect of *Species* on the metabolome of white muscle
190 and red muscle separately. The effects of *Storage condition* on-board purse-seiners (i.e., brine- vs
191 deep-freezing) and *Geographical origin* (i.e., MOZ vs WCIO) were also investigated for each
192 species and muscle type. Finally, the effect of *Size category* was considered for YFT and BET

193 only: two distinct size categories were taken into account, based on YFT and BET life history
194 traits (i.e., small tunas < 80 cm FL vs large tunas > 80 cm FL, with FL=80 cm corresponding to
195 the size at which YFT and BET reach their size-at-first maturity, change their aggregative
196 behaviour and habitat from surface to deeper waters and thus their diet; (Chassot et al., 2019,
197 2015; Sardenne, Bodin, et al., 2016)). SKJ is a smaller tuna species than YFT and BET
198 (maximum length of 110 cm for SKJ compared to 230 cm for YFT and BET), and does not show
199 specific behavioural changes with size being aggregated in schools near the surface through their
200 lifespan. For this reason, the factor Size category was not considered for SKJ. A PCA was first
201 performed to reveal intrinsic clusters and detect potential outliers. PLS-DA was then used to
202 model the relationship between groups and spectral data. Before analysis, the orthogonal signal
203 correction filtering was applied to remove variation not linked to the factors of interest
204 (physiological, experimental, or instrumental variation). Filtered data were mean-centred and
205 scaled (unit variance or Pareto scaling). For the figures, we used Hotelling's T2 statistics to
206 construct 95% confidence ellipses. The goodness-of-fit parameter R²Y parameter represents the
207 explained variance. Seven-fold cross-validation was used to determine the number of latent
208 variables to include in the PLS-DA model and to estimate the predictive ability (Q² parameter) of
209 the adjusted model. The robustness of the PLS-DA regression models was assessed by comparing
210 R²Y and Q²: R²Y varies between 0 and 1, where 1 indicates a perfect fit between the model and
211 the data; When Q² is greater than 0.5, the model is considered to have good predictability, and if
212 Q² is greater than 0.9, then the model is considered to have excellent predictability.

213 In addition, the robustness of the PLS-DA model was assessed using a permutation test (200
214 permutations). Discriminant variables were determined using the VIP (variable importance in the
215 projection) value, a global measure of the influence of each variable on the PLS components.
216 Variables with VIP > 0.8 were considered discriminant. A non-parametric Kruskal–Wallis test
217 was then used to determine which metabolites were significantly different between groups. NMR
218 variables with a p-value <0.05 were considered significantly different. SIMCA-P software (V12;
219 Umetrics AB, Umea, Sweden) was used to perform the multivariate analyses and R software
220 (version 2.12, <http://www.r-project.org>) was used to perform univariate Kruskal-Wallis test.

221

222 **3 Results and discussion**

223 3.1 Identification of tropical tunas' white and red muscle metabolite profiles

224 Both muscles (388 samples) displayed similar metabolites, although changes in the relative
225 intensities of some resonances were observed. Figures 2A and 2B show representative ¹H NMR
226 spectra from white and red muscles of tuna respectively. The assignment of the peaks to specific

227 metabolites was achieved based on the literature and confirmed by 2D COSY and HSQC
228 spectroscopy. The ¹H NMR spectra of tuna muscle samples contained a number of assignable
229 amino acids, organic acids, glucose and lipids, as observed in fish muscle in general (Konosu &
230 Yamaguchi, 1982; Piñeiro et al., 2003). Twenty-five metabolites were identified based on their
231 1D and 2D spectra, and Table 1 lists the compounds assigned. The comparison of tuna muscles
232 spectra allowed for the identification of four groups of signals and related metabolites:

233 *Group I – degradation biomarkers:* The low-field region (8.6-4.4 ppm) of the NMR spectra
234 displays signals belonging to adenosine triphosphate (ATP) degradation products, i.e., inosine,
235 inosine-5-monophosphate (IMP), and hypoxanthine. ATP predominates the nucleotides in muscle
236 of live animals under normal conditions, but after death a series of enzymatic reactions leads to
237 the decomposition of ATP into adenosine diphosphate (ADP), adenosine monophosphate (AMP),
238 inosine monophosphate (IMP), inosine, hypoxanthine, xanthine and ultimately uric acid. When
239 the level of ATP has dropped under a critical level, the muscle enters *rigor mortis*. Moreover,
240 hypoxanthine is a known contributor to the bitter off-flavour of spoiled fish while IMP is usually
241 associated to the desirable taste of fresh fish. The degree of freshness is thus often expressed as
242 the K-value, defined as the ratio of the sum of inosine and hypoxanthine concentrations to the
243 total concentration of ATP metabolites (Karube et al., 1984).

244 *Group II – essential metabolites:* In the mid-field region (5.2-3.2 ppm) of the NMR spectra, the
245 signals of choline and its derivative metabolites, namely phosphoethanolamine (PE) and
246 glycerophosphorylcholine (GPC) were detected. The spectral region is also characterized by the
247 presence of sugar signals (glucose). Choline and its derivatives result from the hydrolysis of
248 phospholipids, in particular of phosphatidylcholine, which are found in high proportions in the
249 lipid fraction of SKJ, YFT and BET (Sardenne et al., 2016b). Involvement of these compounds in
250 aging of samples due to storage conditions has already been pointed out (Scano et al., 2012).
251 Hydrolysis of the ester bond that links the glycerol backbone of lipid molecules to fatty acids
252 results in the release of the latter in their free form, making them more prone to oxidation
253 (Refsgaard et al., 2000) which can be very fast in highly unsaturated fatty acids such as
254 docosahexaenoic acid (DHA) and eicosapentaenoic acid (EPA) present in tuna muscle in high
255 quantity. Therefore, hydrolysis of the lipid molecules makes the food matrix more exposed to
256 oxidation.

257 *Group III – energy expenditure:* The signals with the highest intensity were observed in the low-
258 field and mid-field NMR spectra regions, and assigned to anserine, lactate, creatine and
259 phosphocreatine. Low-intensity signals belonging to carnosine, succinate, and trimethylamine
260 (TMA) were also identified. Creatine and phosphocreatine represent an important energy deposit

261 in skeletal muscle. In fact, most of the creatine is phosphorylated in resting muscle and supplies
262 energy in the form of high energy phosphate for muscular contraction. Fish exposed to stress
263 prior to death have lower values of phosphocreatine and ATP than unstressed fish (Erikson et al.,
264 1997). Moreover, degradation of creatine/phosphocreatine into creatinine/phospho-creatinine
265 through intramolecular cyclization has been reported to be favoured by different chemical–
266 physical conditions including temperature (Chan et al., 1994). Distinct peaks from anserine (β -
267 alanyl-1-methylhistidine) and carnosine (β -alanyl-histidine), the most frequently dipeptides
268 occurring in fish (Abe, 1983; Konosu & Yamaguchi, 1982) were visible in all samples. The high
269 level of anserine observed in tuna muscle is typical for migratory pelagic species (Abe et al.,
270 1986; Konosu & Yamaguchi, 1982). These dipeptides are believed to act as a buffer during
271 anaerobic metabolism, a fact reflected by the high levels in muscles used for burst activity
272 (Boldyrev & Severin, 1990). In addition, anserine and carnosine have been proposed to play
273 additional roles in controlling enzyme activity, inhibiting oxidative reactions, and as
274 neurotransmitter (Boldyrev, 2001; Boldyrev & Severin, 1990). Anserine decomposes into its
275 constituents β -alanine and 1-methylhistidine by hydrolysis. This permitted to estimate the loss of
276 quality during ice storage by measuring the levels of 1-methylhistidine, β -alanine, anserine and
277 tryptophan (Ruiz-Capillas & Moral, 2001). Lactate is typically found in high abundance in tuna
278 muscle as it is involved in burst swimming activity: glucose is broken down and oxidized to yield
279 pyruvate, and lactate is then produced from the pyruvate faster than the body can process it,
280 causing lactate concentrations to rise by a factor 7-20 in tuna muscle after fast swimming/hunting
281 (Guppy et al., 1979). Lactate also plays an important role both in the evolution of the freshness
282 degree and in the formation of an agreeable odour or not (Bramstedt, 1962). Its concentration
283 reflects the initial glycogen stores before death, the fish handling (e.g., duration of the fishing
284 operation), and the extraction procedure.

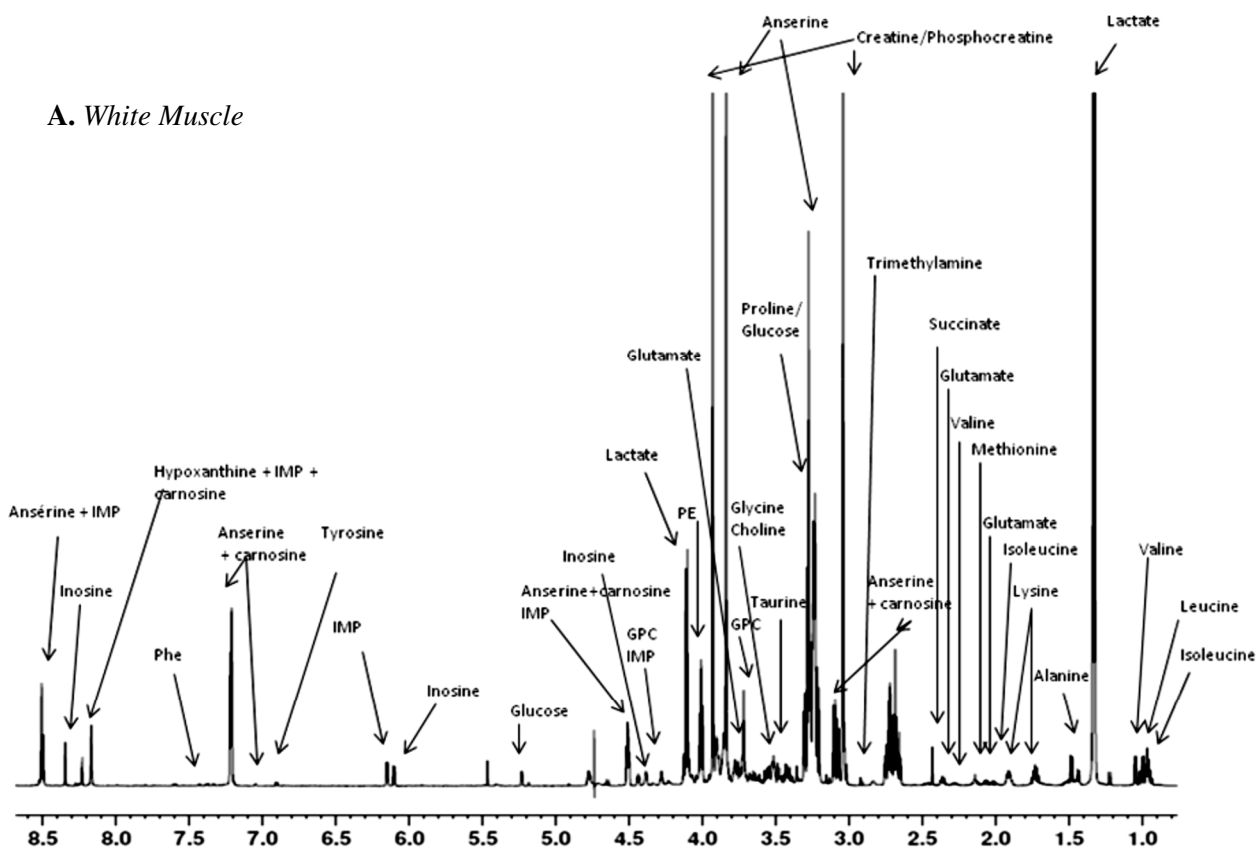
285 *Group IV – muscle structure and its degradation:* The remaining signals in the high-field (3.0-0.9
286 ppm), mid-field (4.2-3.2 ppm) and low-field (6.8-7.5 ppm) NMR spectra regions belongs to the
287 aliphatic groups, with 12 amino acids identified. Tropical tuna muscles are characterized by a
288 relatively low lipid concentration, and a high concentration of proteins and thus their constituents,
289 amino acids (Sardenne et al., 2016b). Indeed, the ^1H -NMR allowed to detect leucine, isoleucine,
290 valine, lysine, alanine, methionine, glycine, taurine, proline, tyrosine, tryptophan, and
291 phenylalanine. Most of these amino acids are free although some might be part of peptides. Large
292 proteins were not visible because their slow tumbling leads to broad signals. Proteins play
293 important roles in physiological functions including osmoregulation and buffering capacity (Van
294 Waarde, 1988); in addition, they contribute to the aroma and flavour of the fish (Konosu &

295 Yamaguchi, 1982), and increase its antioxidant capacity (Chan et al., 1994). During storage and
296 processing, proteins are degraded, and the level of free amino acids and peptides in muscle
297 changes.

298 It is important to underline a low presence of trimethylamine (TMA, peak at 2.89 ppm) in spectra
299 acquired in this study which is in accordance with previous study on Indian Ocean YFT
300 (Jääskeläinen et al., 2019). TMA is a microbial metabolite and it can only be used as an index of
301 spoilage and not as an index of freshness (Jääskeläinen et al., 2019). Development of TMA in
302 seafood depends primarily on the content of the substrate trimethylamine-oxide (TMAO, peak at
303 3.27 ppm) in the fish raw material, which is reduced into TMA by some species in the
304 bacteriological flora of spoiling fish as *Shewanella putrefaciens*, *Photobacterium phosphoreum*,
305 and Vibrionaceae (Gram & Huss, 1996). In frozen fish, this reaction can be replaced by a slow
306 enzymatic transformation to dimethylamine (DMA) and formaldehyde. TMA can also result from
307 the breakdown of choline from phospholipids.

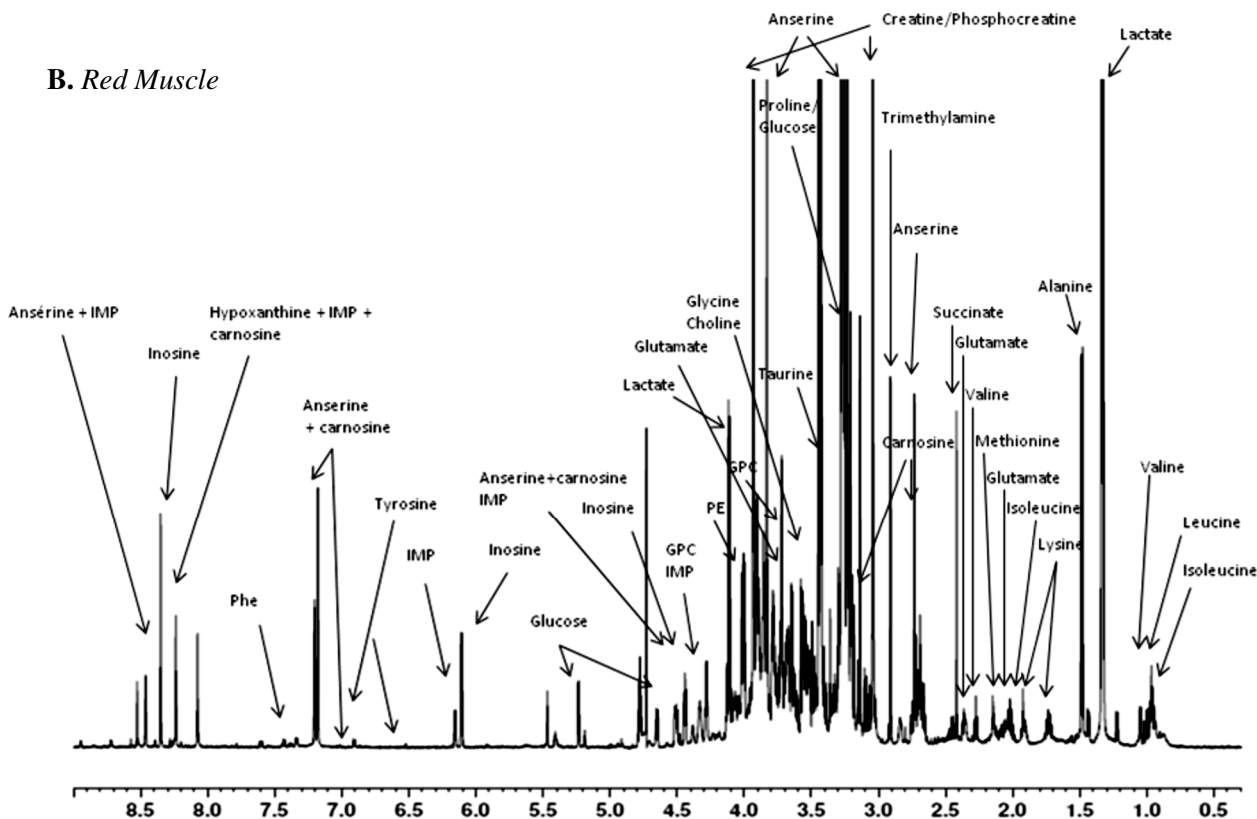
308

A. White Muscle



309

B. Red Muscle



310
311
312
313

Fig. 2. Typical 600 MHz ^1H NMR CPMG spectra from (A) white muscle and (B) red muscle of wild tropical tuna. GPC: Glycerophosphorylcholine; IMP: Inosine-5-monophosphate; Phe: Phenylalanine; PE: Phosphatidylethanolamine.

314 **Table 1.** Representative ¹H-NMR assignments for white and red muscles of wild tropical tuna at 600 MHz. Group indicates the four groups of signals and related
 315 metabolites identified. I – degradation biomarkers; II – essential metabolites; III – energy expenditure; IV – muscle structure and its degradation. Concentration
 316 ranges of metabolites were indicated in blue for white muscle, and in red for red muscle. Concentrations were calculated from proton NMR spectra. NQ means
 317 “non quantifiable”

Metabolite	Concentration range (mM/g muscle)	δ_H ppm (multiplicity, coupling constant, assignment)/ δ_C ppm	Group	Type of metabolite
Inosine (Ino)	0.1-32; 0.1-25	4.29 (m, CH)/88.2; 4.44 (m, CH)/73.1; 6.10 (d, J=5.7 Hz, CH)/90.9; 8.24 (s, CH)/148.9; 8.35 (s, CH)/142.7	I	Nucleoside
Hypoxanthine (Hyp)	NQ	8.21 (s, CH)/135.0; 8.24 (s, CH)/146.2	I	Purine
Inosine-5-monophosphate (IMP)	0.1-34; 0.1-10	8.21 (s, CH)/148.9; 8.54 (s, CH)/142.6; 6.15 (d, J=5.7 Hz, CH)/89.9; 4.38 (m, CH)/87.1	I	Enzyme
Lactate (Lac)	47-778 ; 32-608	1.32 (d, J=6.9 Hz, CH ₃)/22.9; 4.11 (q, J=6.9 Hz, CH)/71.4	II	Organic Acid
Glycerophosphorylcholine (GPC)	0.1-15; 1-47	3.21 (s, N(CH ₃) ₃)/56.6; 3.64 (m, CH ₂)/64.6; 4.30(m, CH ₂)/62.1	II	Essential nutrient
Choline (Cho)	2-32; 2-38	3.22 (s, N(CH ₃) ₃)/56.7; 3.52 (m, CH ₂)/70.1; 4.08 (m, CH ₂)/58.5	II	Essential nutrient
Glucose (Glu)	0.3-35; 0.2-58	3.24 (m, CH) /76.9; 3.40 (m, CH)/72.3; 3.50 (m, CH)/74.2; 3.73 (m, CH)/63.3; 3.91 (m, CH ₂)/63.4; 4.65 (d, J=7.9 Hz, CH)/98.7; 5.24 (d, J=3.7 Hz, CH)/94.9	II	Monosaccharide
Phosphatidylethanolamine (PE)	5-165 ; 3-90	4.02 (m)	II	Phospholipids
Succinate (Suc)	0.1-16 ; 0.7-21	2.42 (s, CH ₂)/36.8	III	Organic Acid
Anserine (Ans)	4-235; 4-106	2.67 (m, CH ₂)/34.8; 3.08 (dd, CH ₂)/28.3; 3.24 (m, CH ₂)/38.3; 3.84 (s, CH ₃)/35.2; 4.51 (dd, CH)/56.1; 7.16 (s, CH)/122.8; 8.35 (s, CH)/138.4	III	Dipeptide
Carnosine (Car)	0-60; 0-33	2.68 (m, CH ₂)/34.8; 3.08 (dd, CH ₂)/30.8; 3.24 (m, CH ₂)/38.6; 4.51 (m, CH, ring)/57.6; 7.06 (s, CH, ring)/119.9; 8.17(s CH, ring)/137.4	III	Dipeptide
Trimethylamine (TMA)	0-1 ; 0.5-14	2.91 (s, N(CH ₃) ₃)/47.5	III	Amine
Creatine/phosphocreatine (Crt/P-crt)	13-213 ; 10-137	3.04 (s, CH ₃)/39.5; 3.93 (s, CH ₂)/66.4	III	Organic Acid
Isoleucine (Ile)	0.1-21 ; 0.4-18	0.94 (t, J=7.4 Hz, CH ₃)/13.9	IV	Amino acid
Leucine (Leu)	0.1-42 ; 0.8-37	0.96 (t, J=5.9 Hz, CH ₃)/23.6	IV	Amino acid
Valine (Val)	0.2-34; 0.7-23	0.99 (d, J=7.0 Hz, CH ₃)/19.4; 1.05 (d, J=7.0 Hz, CH ₃)/20.8; 2.28 (m, CH)/31.9	IV	Amino acid
Alanine (Ala)	0.5-47 ; 3-57	1.48 (d, J=7.1 Hz, CH ₃)/18.9; 3.78 (q, J=7.2 Hz, CH)/53.1	IV	Amino acid
Lysine (Lys)	0.1-17 ; 0.8-28	1.73 (m, CH ₂)/29.2; 1.92 (m, CH ₂)/32.7	IV	Amino acid
Proline (Pro)	NQ	2.04 (m, CH ₂)/32.1; 2.36 (m, CH ₂)/31.7; 3.35 (m, CH ₂)/48.9; 4.13 (m,	IV	Amino acid

Glutamate (Glu)	0.2-31 ; 2-34	CH)/64.0 2.07 (m, CH ₂)/29.6; 2.37 (m, CH ₂)/36.1; 3.78 (m, CH)/56.7	IV	Amino acid
Methionine (Met)	NQ	2.13 (m, CH ₃ / CH ₂)/32.7	IV	Amino acid
Taurine (Tau)	0.7-34 ; 22-337	3.26 (t, J=7.3 Hz, CH ₂)/50; 3.44 (t, J=7.3 Hz, CH ₂)/38.1	IV	Amino acid
Glycine (Gly)	0.8-27 ; 5-88	3.57 (s, CH ₂)/44.3	IV	Amino Acid
Tyrosine (Tyr)	0-9; 0.2-7	6.91 (m, CH ring)/118.9; 7.20 (m, CH ring)/133.5	IV	Amino acid
Phenylalanine (Phe)	0-12; 0-12	7.43 (m, CH ring)/131.8; 7.34 (d, J=7 Hz, CH ring)/132.1 7.39 (m, CH, ring)/130.4	IV	Amino acid

318 3.2 Discrimination between tropical tuna species

319 3.2.1. *Effect of Species on ¹H NMR profiles of tuna muscles.*

320

321 The PLS-DA model derived from tunas' OSC-filtered white muscle spectra revealed R²Y and Q²
322 values of 0.70 and 0.70 for two latent components, respectively, indicating good fit and
323 prediction abilities for the PLS regression model. The three tropical tuna species were separately
324 grouped on the PLS-DA score plot with six compounds or types of molecules, responsible for the
325 inter-species discrimination (Fig. S1A, Table S2). Dipeptides (anserine and carnosine) were the
326 highest in BET followed by SKJ and finally YFT. Phospholipids (PE) had the highest levels in
327 SKJ and the lowest levels in BET. Finally, organic acids (creatine, phosphocreatine and
328 succinate) were predominant in YFT, excepted for lactate that showed the highest and lowest
329 levels in SKJ and BET, respectively.

330 Better fits and prediction abilities were obtained with the PLS-DA model derived from tunas'
331 OSC-filtered red muscle spectra (R²Y = 0.84 and Q² = 0.79 for four latent components) showing
332 a clear separation along the first latent component (t[1] axis) between the three tropical tuna
333 species (Fig. S1B). 27 NMR variables were identified, corresponding to 16 compounds or classes
334 of molecules (Table S2), and three NMR variables were not identified (i.e., "unknown").
335 Metabolites from group III (anserine, carnosine, creatine, phosphocreatine, lactate and succinate)
336 and phospholipids (PE) showed similar inter-species differences in the red muscle as previously
337 observed in the white muscle. Additionally, six amino acids contributed to the discrimination of
338 the tropical tuna species: SKJ had the highest levels of isoleucine, leucine, and lysine and the
339 lowest levels of glutamate and valine; BET had the highest levels of glutamate and valine and the
340 lowest levels of taurine; and finally, YFT had the highest levels of taurine and the lowest levels of
341 isoleucine, leucine and lysine. The essential nutrient GPC (group II) was also discriminant with
342 higher levels observed in SKJ than in BET and YFT red muscle. Lastly, fish quality biomarkers
343 (group I: inosine, IMP and hypoxanthine) were predominant in SKJ red muscle followed by YFT
344 and BET.

345

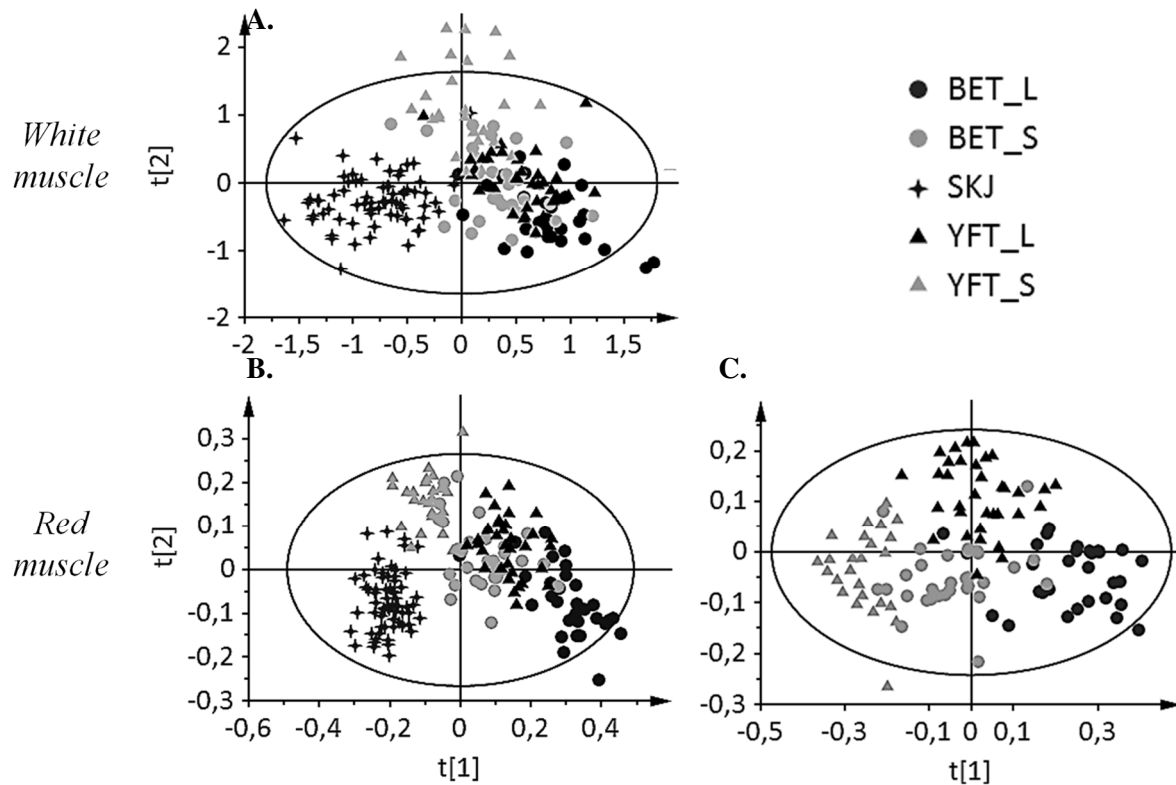
346 3.2.2. *Effect of Species and Size category on ¹H NMR profiles derived from tuna muscles*

347 The PCA score plots derived from the white and red muscle profiles were investigated to
348 differentiate the three tropical tuna species, in particular YFT and BET, taking into account the
349 size category (i.e., small tunas ≤ 80 cm FL versus large tunas ≥ 100 cm FL) of the studied fish
350 (data not shown). Supervised PLS-DA models applied on OSC-filtered revealed R²Y of 0.39 and
351 0.59, Q² values of 0.36 and 0.50 with three and four latent components for the tuna's white and

352 red muscle spectra, respectively, indicating poor fit but good prediction abilities for these PLS
353 regression models. The PLS-DA score plot derived from the OSC-filtered white muscle allowed
354 for the discrimination of SKJ and small YFT only (Fig. 3A). The PLS-DA score plot derived
355 from the red muscle was more discriminant with a clear separation of SKJ, small YFT and large
356 BET, while small BET and large YFT remained confounded (Fig. 3B).

357 Supervised PLS-DA models applied on OSC-filtered data were then applied on the white and red
358 muscle datasets after excluding SKJ data. The derived PLS-DA score plot did not give any valid
359 model ($Q^2 < 0.30$), whereas it allowed for the separation of small and large YFT and BET ($R^2Y =$
360 0.43 and $Q^2 = 0.41$ for two latent components; Fig. 3C). A total of 15 compounds or classes of
361 molecules were identified and one remained unknown, were responsible for the differences
362 between *Species* and *Size category* in the red muscle (Table S3). From the 15 identified chemical
363 species, 13 were common with those responsible for the discrimination of the three tropical
364 species only (Table S2). Differences between SKJ and the two other species were specified when
365 taking into account YFT and BET size categories. Anserine, lactate, succinate, glutamate, and
366 methionine showed similar levels between SKJ and the small YFT and BET but different ones
367 with large tunas; the opposite trends were observed for TMA. Regarding BET versus YFT,
368 valine, anserine and carnosine were predominant in BET and in large individuals compared to
369 small ones for both species. Creatine / phosphocreatine, taurine and lactate were higher in SKJ
370 and in small individuals compared to large ones for YFT, BET and both species respectively.
371 Finally, although no difference was observed between YFT and BET, methionine, TMA and GPC
372 were affected by *Size category* with the large tunas having the highest levels of methionine and
373 TMA and the lowest levels of GPC (for YFT only).

374



376
 377 **Fig. 3** Two-dimensional Partial Least Squares-Discriminant Analysis (PLS-DA) score plots based on the
 378 metabolic profile from white and red muscle aqueous extracts of the three tropical tuna species
 379 categorized by size, i.e., small yellowfin tuna (YFT_S, n=25), large yellowfin tuna (YFT_L, n=35), small
 380 bigeye tuna (BET_S, n=34), large bigeye tuna (BET_L, n=28) and skipjack tuna (SKJ, n=72). (A) PLS-
 381 DA score plot of OSC-filtered integrated ^1H NMR spectra of white muscle extracts for all species/size
 382 categories, using three components ($R^2Y = 0.39$ and $Q^2 = 0.36$); (B) PLS-DA score plot of OSC-filtered
 383 integrated ^1H NMR spectra of red muscle extracts for all species/size categories, using five components
 384 ($R^2Y = 0.59$ and $Q^2 = 0.50$); (C) PLS-DA score plot of OSC-filtered integrated ^1H NMR spectra of red
 385 muscle extracts for four species/size categories only (excluding skipjack), using two components ($R^2Y =$
 386 0.43 and $Q^2 = 0.41$).
 387

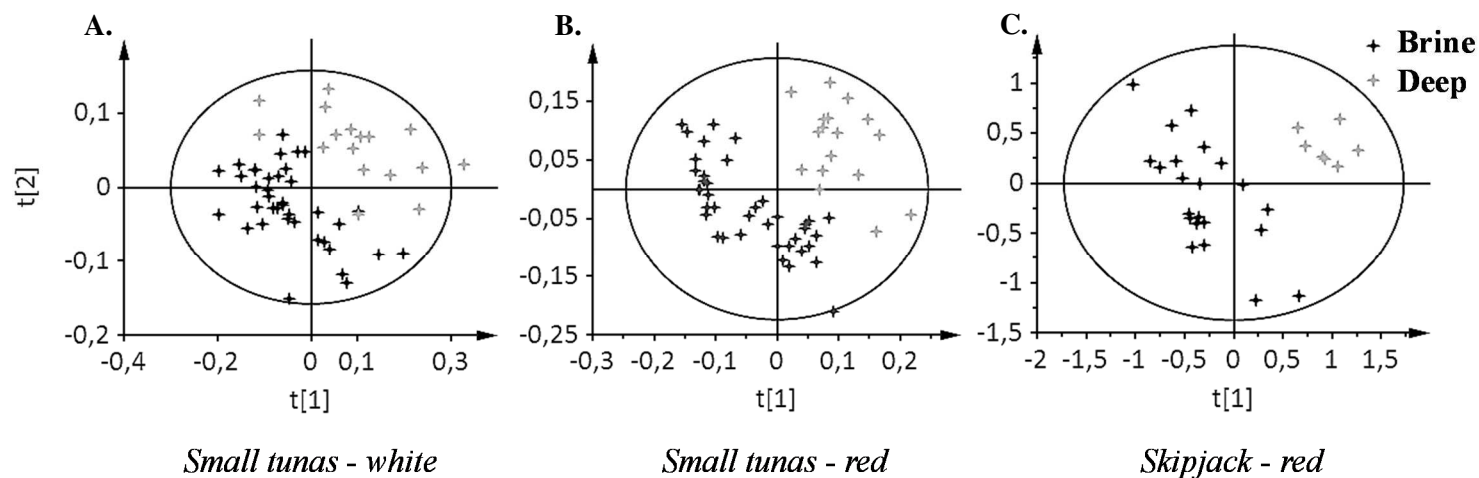
388 3.3 Discrimination of tropical tunas according to storage condition on-board purse seiners

389 The traceability of the tunas' storage conditions on-board purse seiners allowed for the PLS-DA
 390 analysis of the differences in NMR metabolomic profiles from tropical tunas white and red
 391 muscle extracts.

392 The PLS-DA score plot derived from the SKJ and large tuna's OSC-filtered white muscle spectra
 393 as well as from the large tuna's red OSC-filtered muscle spectra did not give any valid model (Q^2
 394 < 0.30), suggesting that both freezing modes affect similarly these size class and species. Only
 395 the white muscle of small tunas (YFT and BET) showed differences between brine-freezing and
 396 deep-freezing storage conditions ($R^2Y = 0.69$ and $Q^2 = 0.46$ for two latent components; Fig. 4A),
 397 with 14 metabolites identified (Table S4). Among them, nine metabolites corresponded to amino
 398 acids that exhibited higher levels in deep-frozen small tunas, most likely reflecting a lower level
 399 of protein degradation during this storage mode. Deep-frozen small tunas were also characterised

400 by lower IMP and higher creatine/phosphocreatine levels compared to brine-frozen ones, which
401 could reflect a slower process of ATP and creatine/phosphocreatine degradation (Chan et al.,
402 1994) .

403 In the red muscle, the freezing storage condition was a discriminant factor for small YFT and
404 BET ($R^2Y = 0.91$ and $Q^2 = 0.82$ for three latent components; Fig. 4B), and SKJ ($R^2Y = 0.79$ and
405 $Q^2 = 0.73$ for one latent component; Fig. 4C). Deep-frozen small tuna's red muscle had higher
406 levels of four amino acids, glycogen and PE, as a result of lower process of degradation; also,
407 from group III, anserine/carnosine and creatine/phosphocreatine were higher in deep-frozen small
408 tunas compared to brine-frozen tunas, while opposite trends were observed for lactate and
409 succinate. Finally, a lower number of metabolites was identified as responsible for the differences
410 between freezing modes (nine against 12 compounds in small tunas' muscles), with PE, anserine,
411 carnosine and glutamate showing higher levels in deep-frozen but lower levels of succinate and
412 taurine compared to brine-frozen SKJ red muscle.



414
415
416
417
418
419
420
421

Fig. 4. Two-dimensional Partial Least Squares-Discriminant Analysis (PLS-DA) score plots based on the metabolic profile from white and red muscle aqueous extracts of the tropical tuna species depending on the storage conditions onboard the purse-seine vessels, i.e., brine-freezing and deep-freezing. (A) PLS-DA score plot of OSC-filtered integrated ^1H NMR spectra of white muscle extracts for small tunas ($n = 83$ and 48 stored in brine- and deep-freezing wells, respectively), using two components ($R^2Y = 0.69$ and $Q^2 = 0.46$); (B) PLS-DA score plot of OSC-filtered integrated ^1H NMR spectra of red muscle extracts for small tunas ($n = 83$ and 48 stored in brine- and deep-freezing wells, respectively), using three components ($R^2Y = 0.91$ and $Q^2 = 0.82$); (C) PLS-DA score plot of OSC-filtered integrated ^1H NMR spectra of red muscle extracts for SKJ ($n = 42$ and 17 stored in brine- and deep-freezing wells, respectively), using one component ($R^2Y = 0.79$ and $Q^2 = 0.73$).

422

423 3.4 Discrimination of the purse seine tropical tunas according to their geographical origin

424 The information on the fishing locations retrieved from the purse-seine logbooks was merged
425 with the NMR metabolomic profiles from tropical tunas white and red muscle extracts and
426 analysed with PLS-DA.

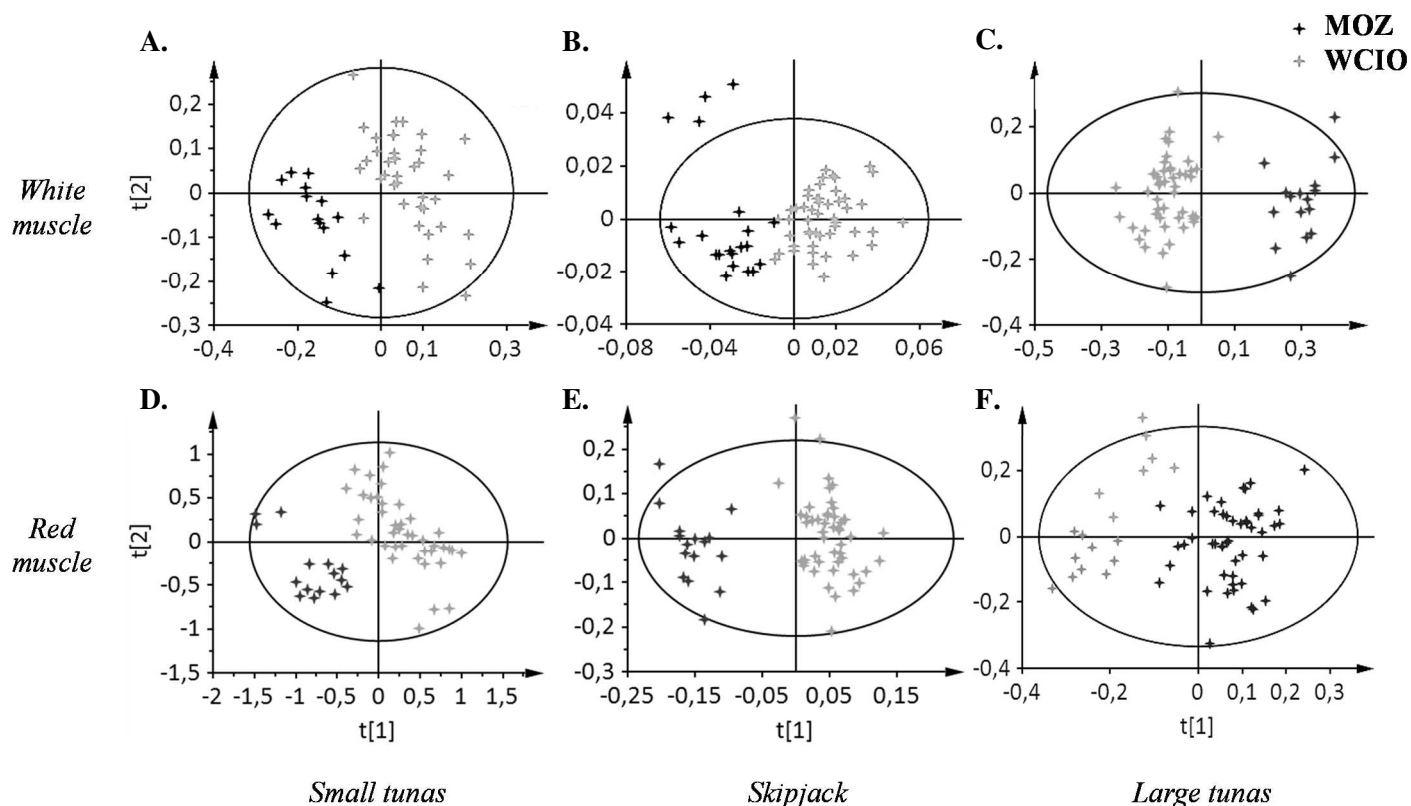
427 Fig. 5A, 5B and 5C represent the PLS-DA score plots derived from the white muscle of small
428 YFT and BET ($R^2Y = 0.82$ and $Q^2 = 0.73$ for two latent components), SKJ ($R^2Y = 0.74$ and $Q^2 =$
429 0.70 for two latent component) and large YFT and BET ($R^2Y = 0.79$ and $Q^2 = 0.77$ for one latent
430 component), respectively. Fig. 5D, 5E and 5F represent the PLS-DA score plots derived from the
431 red muscle of small YFT and BET ($R^2Y = 0.84$ and $Q^2 = 0.73$ for two latent components), SKJ
432 ($R^2Y = 0.89$ and $Q^2 = 0.83$ for one latent component) and large YFT and BET ($R^2Y = 0.85$ and
433 $Q^2 = 0.77$ for three latent component), respectively. All PLS regression models gave good fit and
434 prediction abilities.

435 Nine metabolites were identified in the white muscle of small and large tunas as responsible for
436 the differences between *Geographical origin*, against only six in the white muscle of SKJ. For all
437 species and size categories, most metabolites were pertaining to the groups II and III. Based on
438 the identified and level changes in metabolites, a greater resemblance of NMR profiles was
439 however observed between SKJ and small tunas compared to large tunas. For instance, the
440 geographical origin of the small tunas and SKJ was well distinguished with small tunas from
441 WCIO having higher levels of essential nutrients (choline and PE), lactate, hypoxanthine, IMP
442 and carnosine in white muscle, but lower levels of anserine compared to fish from MOZ (Table
443 S5). Regarding large tunas, the white muscle of WCIO fish was characterised by lower anserine,
444 PE, creatine/phosphocreatine, IMP and carnosine.

445 In the red muscle, 18, 16 and 10 metabolites were contributing to the discrimination of large
446 tunas, small tunas and SKJ respectively, according to the *Geographical origin*. Metabolites
447 belong to groups II, III, and IV for small tunas and SKJ, and to all groups for large tunas. In
448 particular, WCIO large tunas had higher GPC, creatine/phosphocreatine, IMP and inosine but
449 lower TMA, methionine and alanine, and WCIO SKJ had higher choline, isoleucine and leucine,
450 hypoxanthine+IMP+carnosine than their congeners from MOZ. Furthermore, large and small
451 tunas exhibited similar variations for 10 metabolites corresponding to higher taurine and
452 anserine+PE+carnosine, and lower glucose, glycogen, glutamate, isoleucine, leucine, lysine,
453 valine and hypoxanthine+IMP+carnosine in WCIO fish. Fewer similitudes were observed
454 between small tunas and SKJ and between large tunas and SKJ with only four (PE, anserine,

455 carnosine and creatine/phosphocreatine) and one (lactate) similar metabolites variations,
456 respectively.

457 The discrimination of WCIO and MOZ tunas observed in this study may result from differences
458 of trophic and behavioural ecology. Indeed, while tropical tunas feed mainly on fish and squids
459 when inhabiting WCIO waters, crustaceans predominate their diet in MOZ (Chassot et al., 2019).
460 Such “red feed” is often related to fish tissue softening in pelagic species (Huss et al., 1995) and
461 may favour proteolytic breakdown producing low molecular weight peptides and free amino
462 acids. The high occurrence of such metabolites may reduce the commercial acceptability of fish,
463 but also accelerate bacterial spoilage and produce biogenic amines (Biji et al., 2016). Moreover,
464 the lower levels of burst activity markers in MOZ tuna noted in this study could be related to
465 differences of habitat size and schooling behaviour between the two studied areas. In MOZ,
466 tropical tunas (all species/size categories) are mainly associated with fish aggregating devices
467 (FADs) and present a relatively restricted habitat, whereas they are found both in free-swimming
468 schools and aggregated under FADs in WCIO (especially large tunas) where they are able to
469 cover large distances to search for potential preys (Chassot et al., 2019; Fonteneau et al., 2013).



470
471
472
473
474
475
476
477
478
479
480
481

Fig. 5. Two-dimensional Partial Least Squares-Discriminant Analysis (PLS-DA) score plots based on the metabolic profile from white and red muscle aqueous extracts of the tropical tuna species per geographical origin, i.e., Mozambique Channel (MOZ) and western-central Indian Ocean (WCIO). (A) PLS-DA score plot of OSC-filtered integrated ^1H NMR spectra of white muscle extracts for small yellowfin and bigeye tunas ($n = 18$ and 40 in MOZ and WCIO, respectively), using two components ($R^2\text{Y} = 0.82$ and $Q^2 = 0.73$); (B) PLS-DA score plot of OSC-filtered integrated ^1H NMR spectra of white muscle extracts for skipjack ($n = 23$ and 48 in MOZ and WCIO, respectively), using two components ($R^2\text{Y} = 0.74$ and $Q^2 = 0.70$); (C) PLS-DA score plot of OSC-filtered integrated ^1H NMR spectra of white muscle extracts for large yellowfin and bigeye tunas ($n = 11$ and 54 in MOZ and WCIO, respectively), using one component ($R^2\text{Y} = 0.79$ and $Q^2 = 0.77$); (D) PLS-DA score plot of OSC-filtered integrated ^1H NMR spectra of red muscle extracts for small yellowfin and bigeye tunas ($n = 18$ and 40 in MOZ and WCIO, respectively), using two components ($R^2\text{Y} = 0.84$ and $Q^2 = 0.73$); (E) PLS-DA score plot of OSC-filtered integrated ^1H NMR spectra of red muscle extracts for skipjack tuna ($n = 23$ and 48 in MOZ and WCIO, respectively), using one component ($R^2\text{Y} = 0.89$ and $Q^2 = 0.83$); (F) PLS-DA score plot of OSC-filtered integrated ^1H NMR spectra of red muscle extracts for large yellowfin and bigeye tunas ($n = 11$ and 54 in MOZ and WCIO, respectively), using three components ($R^2\text{Y} = 0.85$ and $Q^2 = 0.77$).

482 4 Conclusion

483 In conclusion, high-resolution ^1H NMR spectroscopy of aqueous extracts from white and red
484 muscles of tropical tunas proved to be very efficient for evidencing rich metabolic information
485 (amino acids, dipeptides, organic acids, and other essential nutrients) allowing to discriminate
486 species and size categories, and in a lesser extent on-board storage modes. Discrimination with
487 respect to geographical origin for small tropical tunas was also possible (mainly based on burst
488 activity markers and essential nutrients), which could improve traceability of tuna products in
489 world market. Considering the global scale of this market, geographical comparisons should be
490 extended to the global ocean.

491

492

493 Authors' contribution

494 Conceptualization, NB and HG; Funding Acquisition, NB and EC; Project Administration, NB,
495 HG, LD; Sampling and Data Acquisition, AA, CC, EF, FS and NB; Data Curation and Analysis,
496 AA, CC and MT-F; Writing – Original Draft Preparation, AA and NB; Writing – Review &
497 Editing, All co-authors.

498

499 Acknowledgments

500 This work is a contribution to the project “CANAL: Influence of environmental and biological
501 factors on tuna meat quality” with the financial support of Thai Union Europe Group (ex-
502 MWBrands Ltd). All NMR experiments were performed on the instruments of the MetaToul-
503 AXIOM platform, partner of the national infrastructure of metabolomics and fluxomics:
504 MetaboHUB (MetaboHUB-ANR-11-INBS-0010, 2011). We are grateful to all the people who
505 contributed to the CANAL project. The interactions with staff from Indian Ocean Tuna (IOT)
506 Ltd. and MWBrands were always positive and crucial for data acquisition. We warmly thank
507 particularly François Rossi, Gary Aglaë, Guy Benstrong, Jo Madnack, Paul Lloyd, Clifford
508 Course, Jean-François Feillet, Claire Vitry, Mei Hing Chhan, Ronny Hoareau, Julie Kowlessur,
509 Alain Olivieri and Gaëta Le Colleter for their availability, support and continuous effort to
510 address the project needs despite their respective responsibilities. We are also grateful to the
511 French and Spanish skippers and crews who have always been very interested in the project and
512 helpful for tuna collection and provision of information on fishing and storage conditions aboard
513 vessels. Finally, the tuna sampling strongly benefited from the help of the Seychelles Fishing
514 Authority (SFA) tuna samplers (Jimmy Esparon, Achille Pascal, Elvis “Abdul” Stephen, Darrel
515 Poris, Ronnie Rose, Rodney Rose, Evans Mathiot, Alex Tirant, Mike Lesperance, Mervin

516 Elisabeth, and Patrick Boniface) and the SFA Research Section who gave us easy access to the
517 laboratory facilities.

518

519

520 **References**

521 Abe, H. (1983). Distribution of free l-histidine and related dipeptides in the muscle of fresh-water fishes.

522 *Comparative Biochemistry and Physiology Part B: Comparative Biochemistry*, 76(1), 35–39.

523 [https://doi.org/10.1016/0305-0491\(83\)90167-0](https://doi.org/10.1016/0305-0491(83)90167-0)

524 Abe, H., Brill, R. W., & Hochachka, P. W. (1986). Metabolism of L-Histidine, Carnosine, and Anserine in

525 Skipjack Tuna. *Physiological Zoology*, 59(4), 439–450.

526 Amiel, A., Tremblay-Franco, M., Gautier, R., Ducheix, S., Montagner, A., Polizzi, A., Debrauwer, L., Guillou,

527 H., Bertrand-Michel, J., & Canlet, C. (2020). Proton NMR Enables the Absolute Quantification of

528 Aqueous Metabolites and Lipid Classes in Unique Mouse Liver Samples. *Metabolites*, 10(1), 9.

529 <https://doi.org/10.3390/metabo10010009>

530 Biji, K. B., Ravishankar, C. N., Venkateswarlu, R., Mohan, C. O., & Gopal, T. K. S. (2016). Biogenic amines in

531 seafood: A review. *Journal of Food Science and Technology*, 53(5), 2210–2218.

532 <https://doi.org/10.1007/s13197-016-2224-x>

533 Boldyrev, A. A. (2001). Carnosine as a modulator of endogenous Zn²⁺ effects. *Trends in Pharmacological*

534 *Sciences*, 22(3), 112–113. [https://doi.org/10.1016/S0165-6147\(00\)01648-5](https://doi.org/10.1016/S0165-6147(00)01648-5)

535 Boldyrev, A. A., & Severin, S. E. (1990). The histidine-containing dipeptides, carnosine and anserine:

536 Distribution, properties and biological significance. *Advances in Enzyme Regulation*, 30, 175–194.

537 [https://doi.org/10.1016/0065-2571\(90\)90017-v](https://doi.org/10.1016/0065-2571(90)90017-v)

538 Bramstedt, F. (1962). Amino acid composition of fresh fish and influence of storage and processing. In

539 *Fish in Nutrition* (E. Heen, R. Kreuzer, pp. 61–67).

540 Chan, K. M., Decker, E. A., & Feustman, D. C. (1994). Endogenous skeletal muscle antioxidants. *Critical*

541 *Reviews in Food Science and Nutrition*, 34(4), 403–426.

542 <https://doi.org/10.1080/10408399409527669>

543 Chassot, E., Assan, C., Soto, M., Damiano, A., Delgado de Molina, A., Joachim, L. D., Cauquil, P.,

544 Lesperance, F., Curpen, M., Lucas, J., & Floch, L. (2015). *Statistics of the European Union and*

545 *associated flags purse seine fishing fleet targeting tropical tunas in the Indian Ocean 1981-2014*

546 (Centre IRD de Bondy). *IOTC-2015-WPTT17-12*.

547 <http://www.documentation.ird.fr/hor/fdi:010063283>

548 Chassot, E., Bodin, N., Sardenne, F., & Obura, D. (2019). The key role of the Northern Mozambique

549 Channel for Indian Ocean tropical tuna fisheries. *Reviews in Fish Biology and Fisheries*, 29(3),

550 613–638. <https://doi.org/10.1007/s11160-019-09569-9>

551 Dickson, K. A. (1995). Unique adaptations of the metabolic biochemistry of tunas and billfishes for life in
552 the pelagic environment. *Environmental Biology of Fishes*, 42(1), 65–97.
553 <https://doi.org/10.1007/bf00002352>

554 Erikson, U., Beyer, U. R., & Sigholt, T. (1997). Muscle high-energy phosphates and stress affect K-values
555 during ice storage of Atlantic salmon (*Salmo salar*). *Journal of Food Science*, 62(1), 43–47.
556 <https://doi.org/10.1111/j.1365-2621.1997.tb04365.x>

557 FAO. (2020). *The State of World Fisheries and Aquaculture 2020. Sustainability in action*. Food and
558 Agriculture Organization of the United Nations. <https://doi.org/10.4060/ca9229en>

559 Fonteneau, A., Chassot, E., & Bodin, N. (2013). Global spatio-temporal patterns in tropical tuna purse
560 seine fisheries on drifting fish aggregating devices (DFADs): Taking a historical perspective to
561 inform current challenges. *Aquatic Living Resources*, 26(01), 37–48.
562 <https://doi.org/10.1051/alr/2013046>

563 Gram, L., & Huss, H. H. (1996). Microbiological spoilage of fish and fish products. *International Journal of*
564 *Food Microbiology*, 33(1), 121–137. [https://doi.org/10.1016/0168-1605\(96\)01134-8](https://doi.org/10.1016/0168-1605(96)01134-8)

565 Guppy, M., Hulbert, W. C., & Hochachka, P. W. (1979). Metabolic Sources of Heat and Power in Tuna
566 Muscles: II. Enzyme and Metabolite Profiles. *Journal of Experimental Biology*, 82(1), 303–320.

567 Hatzakis, E. (2019). Nuclear Magnetic Resonance (NMR) Spectroscopy in Food Science: A Comprehensive
568 Review. *Comprehensive Reviews in Food Science and Food Safety*, 18(1), 189–220.
569 <https://doi.org/10.1111/1541-4337.12408>

570 Huss, H. H. (ed), Boerresen, T., Dalgaard, P., Gram, L., Jensen, B., Joergensen, B., Nielsen, J., Baek Olsen,
571 K., Gill, T., & Lupin, H. M. (1995). Quality and quality changes in fresh fish. *FAO Fisheries*
572 *Technical Paper, No 348*, 203.

573 IOTC Secretariat. (2019). *Report of the 21st session of the IOTC Working Party on Tropical Tunas. IOTC-*
574 *2019-WPTT21-R*, 142.

575 Jääskeläinen, E., Jakobsen, L. M. A., Hultman, J., Eggers, N., Bertram, H. C., & Björkroth, J. (2019).
576 Metabolomics and bacterial diversity of packaged yellowfin tuna (*Thunnus albacares*) and
577 salmon (*Salmo salar*) show fish species-specific spoilage development during chilled storage.
578 *International Journal of Food Microbiology*, 293, 44–52.
579 <https://doi.org/10.1016/j.ijfoodmicro.2018.12.021>

580 Jung, Y., Lee, J., Kwon, J., Lee, K.-S., Ryu, D. H., & Hwang, G.-S. (2010). Discrimination of the Geographical
581 Origin of Beef by ¹H NMR-Based Metabolomics. *Journal of Agricultural and Food Chemistry*,
582 58(19), 10458–10466. <https://doi.org/10.1021/jf102194t>

583 Karube, I., Matsuoka, H., Suzuki, S., Watanabe, E., & Toyama, K. (1984). Determination of fish freshness
584 with an enzyme sensor system. *Journal of Agricultural and Food Chemistry*, 32(2), 314–319.
585 <https://doi.org/10.1021/jf00122a034>

586 Konosu, S., & Yamaguchi, K. (1982). The flavor components in fish and shellfish. In *Chemistry and*
587 *biochemistry of marine food products* (R. E. Martin, G. J. Flick, C. E. Hebard, & D. R. Ward, pp.
588 367–404).

589 Martinez, I., Bathen, T., Standal, I. B., Halvorsen, J., Aursand, M., Gribbestad, I. S., & Axelson, D. E. (2005).
590 Bioactive Compounds in Cod (*Gadus morhua*) Products and Suitability of ¹H NMR Metabolite
591 Profiling for Classification of the Products Using Multivariate Data Analyses. *Journal of*
592 *Agricultural and Food Chemistry*, 53(17), 6889–6895. <https://doi.org/10.1021/jf0507902>

593 Medina, I., Sacchi, R., & Aubourg, S. (2000). Application of ¹³C NMR to the selection of the thermal
594 processing conditions of canned fatty fish. *European Food Research and Technology*, 210(3),
595 176–178. <https://doi.org/10.1007/pl00005508>

596 Nielsen, E. E., Cariani, A., Aoidh, E. M., Maes, G. E., Milano, I., Ogden, R., Taylor, M., Hemmer-Hansen, J.,
597 Babbucci, M., Bargelloni, L., Bekkevold, D., Diopere, E., Grenfell, L., Helyar, S., Limborg, M. T.,
598 Martinsohn, J. T., McEwing, R., Panitz, F., Patarnello, T., ... Carvalho, G. R. (2012). Gene-
599 associated markers provide tools for tackling illegal fishing and false eco-certification. *Nature*
600 *Communications*, 3(1), 851. <https://doi.org/10.1038/ncomms1845>

601 Pecoraro, C., Zudaire, I., Bodin, N., Murua, H., Taconet, P., Díaz-Jaimes, P., Cariani, A., Tinti, F., & Chassot,
602 E. (2016). Putting all the pieces together: Integrating current knowledge of the biology, ecology,
603 fisheries status, stock structure and management of yellowfin tuna (*Thunnus albacares*). *Reviews*
604 *in Fish Biology and Fisheries*, 1–31. <https://doi.org/10.1007/s11160-016-9460-z>

605 Picone, G., Balling Engelsen, S., Savorani, F., Testi, S., Badiani, A., & Capozzi, F. (2011). Metabolomics as a
606 Powerful Tool for Molecular Quality Assessment of the Fish *Sparus aurata*. *Nutrients*, 3(2), 212–
607 227. <https://doi.org/10.3390/nu3020212>

608 Piñeiro, C., Barros-Velázquez, J., Vázquez, & Figueras, A. (2003). Proteomics as a Tool for the
609 Investigation of Seafood and Other Marine Products. *Journal of Proteome Research*, 2(2), 127–
610 135. <https://doi.org/10.1021/pr0200083>

611 Refsgaard, H. H. F., Brockhoff, P. M. B., & Jensen, B. (2000). Free Polyunsaturated Fatty Acids Cause Taste
612 Deterioration of Salmon during Frozen Storage. *Journal of Agricultural and Food Chemistry*,
613 48(8), 3280–3285. <https://doi.org/10.1021/jf000021c>

614 Ruiz-Capillas, C., & Moral, A. (2001). Changes in free amino acids during chilled storage of hake
615 (*Merluccius merluccius* L.) in controlled atmospheres and their use as a quality control index.
616 *European Food Research and Technology*, 212(3), 302–307.
617 <https://doi.org/10.1007/s002170000232>

618 Sacchi, Raffaele., Medina, Isabel., Aubourg, S. P., Giudicianni, Italo., Paolillo, Livio., & Addeo, Francesco.
619 (1993). Quantitative high-resolution carbon-13 NMR analysis of lipids extracted from the white

620 muscle of Atlantic tuna (*Thunnus alalunga*). *Journal of Agricultural and Food Chemistry*, 41(8),
621 1247–1253. <https://doi.org/10.1021/jf00032a016>

622 Samuelsson, L. M., & Larsson, D. G. J. (2008). Contributions from metabolomics to fish research.
623 *Molecular BioSystems*, 4(10), 974–979. <https://doi.org/10.1039/B804196B>

624 Sardenne, F., Bodin, N., Chassot, E., Amiel, A., Fouché, E., Degroote, M., Hollanda, S. J., Pethybridge, H.,
625 Lebreton, B., Guillou, G., & Ménard, F. (2016a). Trophic niches of sympatric tropical tuna in the
626 Western Indian Ocean inferred by stable isotopes and neutral fatty acids. *Progress in*
627 *Oceanography*, 146, 75–88. <https://doi.org/10.1016/j.pocean.2016.06.001>

628 Sardenne, F., Chassot, E., Fouché, E., Ménard, F., Lucas, V., & Bodin, N. (2016b). Are condition factors
629 powerful proxies of energy content in wild tropical tunas? *Ecological Indicators*, 71, 467–476.
630 <https://doi.org/10.1016/j.ecolind.2016.06.031>

631 Sardenne, F., Kraffe, E., Amiel, A., Fouché, E., Debrauwer, L., Ménard, F., & Bodin, N. (2017). Biological
632 and environmental influence on tissue fatty acid compositions in wild tropical tunas.
633 *Comparative Biochemistry and Physiology Part A: Molecular & Integrative Physiology*, 204, 17–
634 27. <https://doi.org/10.1016/j.cbpa.2016.11.007>

635 Scano, P., Rosa, A., Locci, E., Manzo, G., & Dessì, M. A. (2012). Modifications of the ¹H NMR metabolite
636 profile of processed mullet (*Mugil cephalus*) roes under different storage conditions. *Magnetic*
637 *Resonance in Chemistry*, 50(6), 436–442. <https://doi.org/10.1002/mrc.3819>

638 Van Waarde, A. (1988). Biochemistry of non-protein nitrogenous compounds in fish including the use of
639 amino acids for anaerobic energy production. *Comparative Biochemistry and Physiology Part B:*
640 *Comparative Biochemistry*, 91(2), 207–228. [https://doi.org/10.1016/0305-0491\(88\)90136-8](https://doi.org/10.1016/0305-0491(88)90136-8)

641 Watson, R., & Pauly, D. (2001). Systematic distortions in world fisheries catch trends. *Nature*, 414(6863),
642 534–536. <https://doi.org/10.1038/35107050>

643 Wei, F., Fukuchi, M., Ito, K., Sakata, K., Asakura, T., Date, Y., & Kikuchi, J. (2020). Large-Scale Evaluation of
644 Major Soluble Macromolecular Components of Fish Muscle from a Conventional ¹H-NMR
645 Spectral Database. *Molecules*, 25(8), 1966. <https://doi.org/10.3390/molecules25081966>

646